

Inferring material properties in robotic bone drilling processes

JORGE JUAN GIL^{1*}, IÑAKI DÍAZ², FERNANDO ACCINI²

¹ University of Navarra, TECNUN, School of Engineering, San Sebastián, Spain.

² CEIT, Materials and Manufacturing Division, San Sebastián, Spain.

Purpose: Recent innovations in robotics have enabled the development of automatic bone drilling tools which allows surgeons to improve the precision of their surgical operations. However, these tools still lack valuable tactile information about the material properties of the bone, preventing surgeons from making decisions while operating. The aim of this work is to explore whether robotic drilling tools can infer bone condition on the basis of certain key measures, particularly thrust force. **Methods:** To infer material properties in robotic bone drilling processes 1) a complete database of experimental operations with an automatic bone drilling tool is implemented and 2) binary logistic regression models are developed to estimate the type of material from the observed values (mainly the central tendency of the thrust force). This work compares three different materials: bovine bone specimens, porcine bone specimens and Full-Cure 720, which is a general-purpose resin with, *a priori*, much less feed resistance. The DRIBON automatic bone drilling tool developed at CEIT is used for the experiments. **Results:** The classification matrices derived using the logistic models show that it is possible to recognize a bovine bone vs. a porcine bone with a relatively high success rate rate (approximately 90%). In contrast, it is possible to recognize bone material vs. another material (in our case a resin) with a 100% of success. These results are successfully implemented in a new hand-held version of DRIBON. **Conclusions:** We propose a method and devise a novel hand-held tool which show that robotic systems can effectively infer bone material properties.

Key words: method to infer material properties, bone drilling, assisted surgery

1. Introduction

Drilling is a common procedure in bone surgery. It is used in orthopedic surgeries for fractures and bone reconstruction [7], in neurological surgeries, such as craniotomy and stereotactic surgery [11] and in ear surgeries, such as a cochleostomy for cochlear implantation [20]. The objective of the surgeon while drilling a bone is to drill holes with the depth and diameter required for the surgical procedure while avoiding any possible mechanical or thermal damage to the bone [6], and being cautious about not damaging any surrounding tissue. Currently, the drilling process is done manually by the surgeon. The accuracy and precision with which the holes are drilled depends to a considerable extent on the experience

and dexterity of the surgeon, and their “drilling by feeling” [5].

In order to improve the safety and accuracy of bone drilling procedures, many automatic drilling prototypes have been developed [4], [8], [9], [12], [13], [15]. Nevertheless, in general, surgeons are reluctant to use such robotic systems because, unlike the manual procedure, they do not offer tactile feedback that allows them to infer, for example, the state of the bone (*e.g.*, healthy or weak bone). If the bone is unhealthy, for example, the screws for orthopedic surgeries cannot be mounted.

The aim of the present work is to try to infer some of the information, specifically information related to the condition of the bone, through an automatic bone drilling tool, in order to support safer and more precise operations. We propose a bone state awareness

* Corresponding author: Jorge Juan Gil, University of Navarra, TECNUN, School of Engineering, Paseo de Manuel Lardizábal 13, 20018 Donostia – San Sebastián, Spain. E-mail: jjgil@tecnun.es

Received: May 20th, 2019

Accepted for publication: July 22nd, 2019

method that is based on a statistical analysis of the thrust force. Thrust force is analyzed as a parameter that is directly related to the mechanical feed resistance of the material. This resistance depends on the material being drilled and/or the condition of the material (e.g., weaker due to some anomaly). One of the drawbacks of using this parameter is that its value greatly depends on other parameters: feed rate, drill rotational speed, drill bit, bone type, etc. The present work implements a large database of experimental thrust force values that depend on different feed rates and drill rotational speed values to determine in real-time whether bone resistance lies in the normal range.

The paper is organized as follows: in Chapter 2, the method to create a database of thrust force values for a set of specific operating conditions and bone specimens is described, and in Chapter 3, the results of the average thrust force are presented. The ability of logistic regression models for inferring bone properties from the database values is discussed in Chapter 4, and in Chapter 5, the new hand-held version of the DRIBON system is described, which implements the bone state awareness feature proposed in this work. Finally, in Chapter 6, conclusions of the study are gathered.

2. Materials and methods

In the literature, many of the authors that have developed bone drilling mechatronic devices have done their trials with bovine and porcine bones [4], [8], [12], [16], [17], based on the assumption that the mechanical properties of both types of bones are similar to those of human bones. Thus, it is reasonable to assume that the mechanical properties of both types of bones are also similar to each other. In this work, both bovine and porcine bones were used for the experiments instead of human bones, and their differences (if any) were analyzed. Results will allow for discussing this assumption with quantitative data.

Ideally, the mean thrust force recorded during the drilling process would indicate whether the resultant hole can properly accommodate a screw or whether the bone presents an anomaly. In the case that the mean thrust force does not correspond to what is expected, the discrepancies may be due to the presence of a bone with anomalies (e.g., the presence of osteoporosis). To check that the system is able to detect these anomalies, we also ran experiments on a mate-

rial that has lower mechanical resistance. We selected FullCure 720, a general-purpose resin.

2.1. Experimental setup

The DRIBON automatic bone drilling tool developed at CEIT will be used for the experiments (Fig. 1). The system is able to drill within a feed rate of 0 to 2 mm/s, a rotational speed from 0 to 3500 rpm and an effective thrust force from 0 to 70 N. The device is designed to perform drilling operations automatically and stop the process just before breakthrough occurs by using only the information provided by a position sensor [17]. The control algorithm consists of a proportional controller with saturation [2]. The input reference for the algorithm is a ramp signal with slope v_r , which imposes a constant feed rate on the tool.

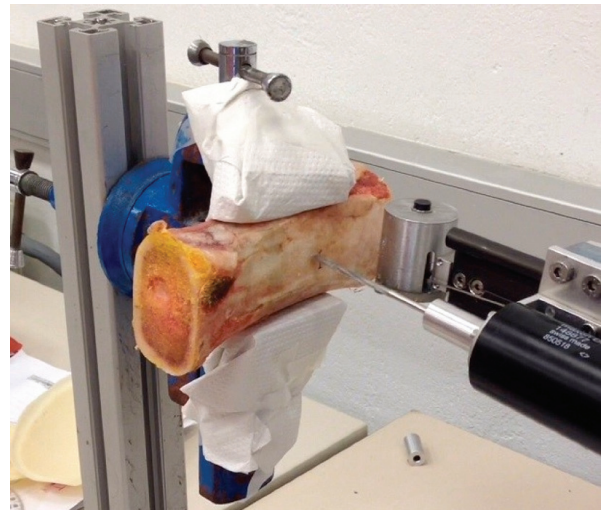


Fig. 1. DRIBON system drilling a bovine bone

Although DRIBON does not include a force sensor, the effective thrust force can be approximated by the force commanded by the controller, because the friction of the device is very small and the inertial force is negligible. The accuracy of this estimation was validated by comparing the estimated force profiles using DRIBON and the thrust forces recorded in a computer numerical control (CNC) machine [1]. Thus, during the drilling process, our device can record and display online the following operating parameters: rotational speed ω_r , feed rate v_r and commanded thrust force f .

To develop the thrust force database, drilling experiments were performed in 10 bone specimens, 5 bovine and 5 porcine samples (0–24 months old). Bones were collected on different days from a butcher and were immediately used for the experiments. Each

specimen was held in place with a c-clamp (Fig. 1). In total, 160 holes were drilled, 80 in each specimen type (16 holes per sample). With the resin FullCure 720, 160 holes were drilled (10 resin pieces, 16 samples).

All the experiments were performed with a surgical twist drill of 3.2 mm diameter and point angle of 90°. In order to reduce the variability in the results obtained due to the wear of the drill bit, a new drill bit was used for each bone sample. Regarding the operating parameters, the feed rate was set to 0.5 and 1 mm/s, and four different rotational speeds were tested: 1500, 2000, 2500 and 3000 rpm. For each combination of feed rate v_r [mm/s] and rotational speed ω_r [rpm], two tests were performed (16 holes per sample). These operating conditions were defined based on the records found in the literature [19] and suggestions of surgeons from the Clínica Universidad de Navarra, who consider these values to be common inside an operating room.

The acquisition rate was set to 1 kHz. The bone drilling process was automatically stopped in each experiment prior to breakthrough of the first cortical layer.

2.2. Obtaining the average thrust force

If the thrust force required to drill the cortical layer of the bone is constant, the force profile recorded by DRIBON exhibits a particular shape (Fig. 2). Outside the bone, the controller only overcomes the friction of the tool (f_r). When the drill bit comes into contact with the bone, the proportional controller behaves like a spring, increasing the force as the error increases. Once the required thrust force is reached, the commanded force (f) is constant throughout the rest of the cortical layer.

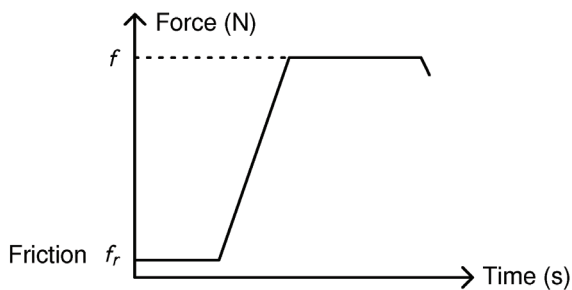


Fig. 2. Profile of the commanded force using DRIBON

In Figure 3 two graphics with the data obtained from two experiments are shown: one with a bovine bone and one with a porcine bone. In the upper plot, the feed rate imposed to the system can be observed,

which in the two examples is 1 mm/s, versus the real displacement of the tool in millimeters. In the lower plot, the commanded thrust force is shown.

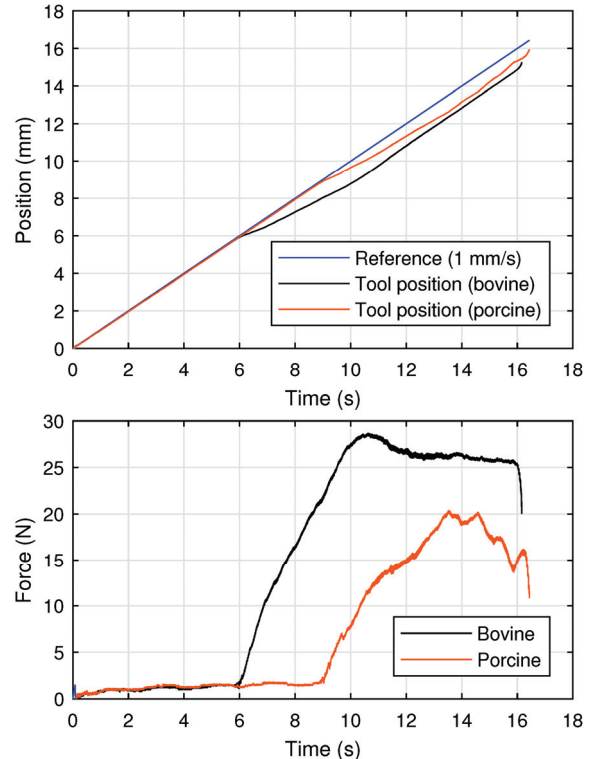


Fig. 3. Experiment data from drilling a bovine specimen with DRIBON: (top) feed rate and actual displacement of the tool; (bottom) estimated force

In cases such as the bovine specimen (black line in Fig. 3), the required thrust force is almost constant and the drill bit reaches nearly constant speed and error inside the cortical wall. However, in other cases, such as the porcine specimen (red line in Fig. 3), it may occur that the required thrust force is not constant and the system advances with small fluctuations around the reference feed rate. Therefore, it is necessary to establish a protocol to determine the effective thrust force for each experiment. In this paper, three measures of the central tendency are considered:

- The arithmetic mean μ_1 of the thrust forces above a friction threshold.
- A weighted average μ_2 of the thrust forces above a friction threshold.
- The median m of the thrust forces above a friction threshold.

The friction threshold was experimentally set at 2.5 N (Fig. 3). Mean value μ_1 can be easily computed by DRIBON during the drilling process. However, this measure is sensitive to the force-rising transient and the thickness of the layer. The median is a more robust measure because it is not skewed so much by

extremely large or small values, and thus it is a better estimation of the effective thrust force. The weighted average μ_2 is computed as follows

$$\mu_2 = \frac{\sum w_k f_k}{\sum w_k}, \quad (1)$$

penalizing the force values that are associated to advance rates different to the reference feed rate v_r . The weighting factors were calculated by the exponential function

$$w_k = e^{-\alpha v_k^2}, \quad (2)$$

where v_k is the derivative of force at time k . Factor w_k is equal to 1 if $v_k = 0$. However, w_k takes a value closer to zero as v_k increases.

3. Results

In Figure 4 the result of the three measures for the porcine specimen experiment shown in Fig. 3 is depicted. It is difficult to know a priori which measure captures better the average thrust force within the cortical layer, or which is better to discriminate the material. This question was analyzed in Section 4.

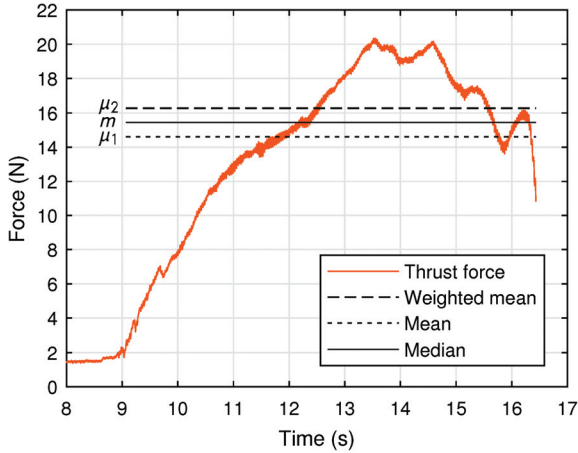


Fig. 4. Mean, median and weighted mean for the thrust force profile of a porcine bone

In Figures 5 and 6 the boxplot of the weighted averages μ_2 of all the experiments with the three materials for each set of parameters: rotational speed and feed rate is shown. The mean and the median measures present quite similar plots, but with slightly different force levels. Since there is a significant overlap between bovine and porcine specimens, it seems difficult to discriminate both types of bones using any of the measures of the average thrust force.

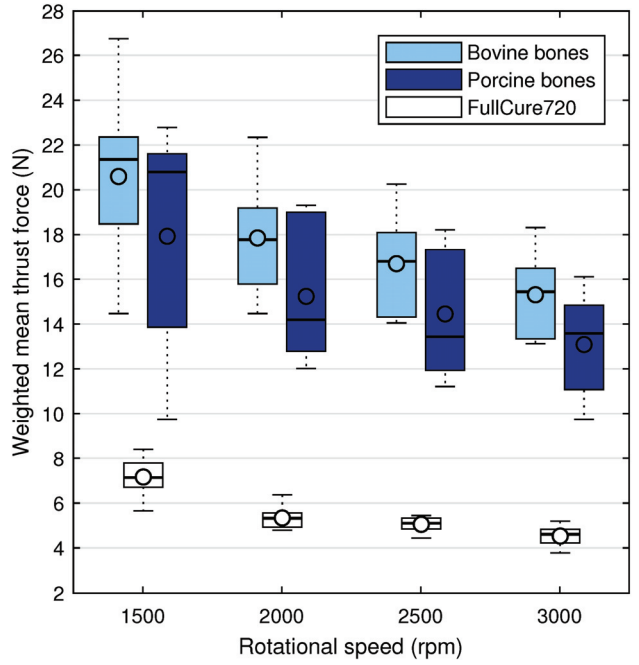


Fig. 5. Boxplot of the weighted mean thrust forces for the three different materials with feed rate of 0.5 mm/s

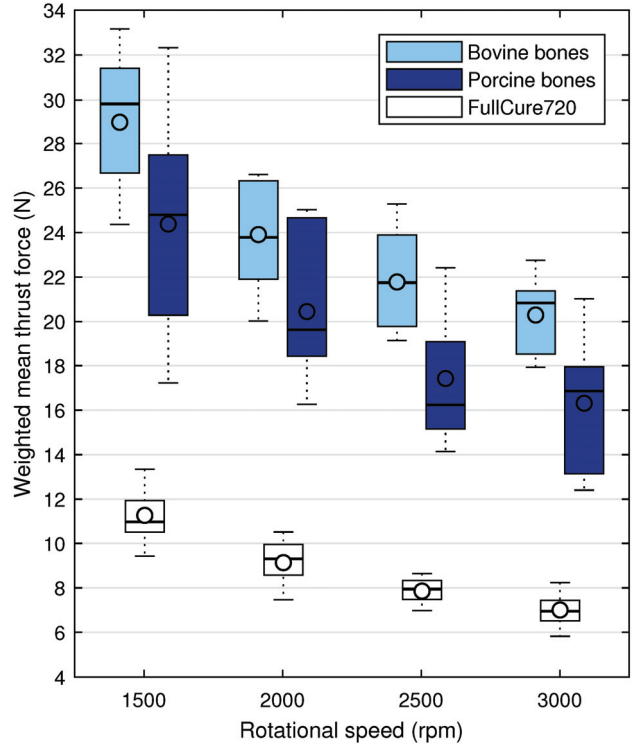


Fig. 6. Boxplot of the weighted mean thrust forces for the three different materials with feed rate of 1 mm/s

The resin with lower mechanical resistance require significantly smaller thrust forces. Additionally, the dispersion of the results is also significantly smaller, or, in other words, the FullCure 720 is a more homogeneous material than bones.

4. Discussion

In this section it is discussed whether it is possible to infer material properties using the thrust force measures collected from the experiments by using binary logistic regression models. It also analyzes which of the proposed measures for the average thrust force achieves better results.

4.1. Bone type recognition

A binary logistic regression model is built to discriminate the type of bone (bovine vs. porcine). The observed outcome for the dependent variable can take only two values: 0 and 1, which represent bovine bone and porcine bone, respectively. The logistic model that estimates the probability of the binary response y based on only one predictor, the thrust force f , is:

$$y \sim \beta_0 + \beta_1 f. \quad (3)$$

In this model, f can be one of the three measures of the effective thrust force: μ_1 , μ_2 and m . Since the

experiments were performed at different rotational speeds ω_r and feed rates v_r , these variables can interact with the thrust force:

$$y \sim \beta_0 + \beta_1 f + \beta_2 (f \times \omega_r) + \beta_3 (f \times v_r). \quad (4)$$

Rotational speed and feed rate are not used as predictors that have a direct effect in the logistic model (4) since they were imposed in the experiments. In other words, it does not make physical sense to include a direct effect of rotational speed and feed rate in the model because they do not change with bone type. The model tries to identify the bone specimen based on the measure of the thrust force, which can also be affected by the rotational speed and the feed rate.

In Table 1 the coefficients and p values of the model using the different measures for the thrust force are shown. Notice that both the rotational speed and the feed rate are taken as factors, while the thrust force is a numerical variable. In principle, the preferred model is the one with minimum AIC value (Akaike information criterion [3]), that is, the one using the median measure.

Table 1. Coefficients and p values of the models

Thrust force using mean measure μ_1					
AIC: 186.32	Coefficient	Estimate	Std. Error	t value	p value
(Intercept)		2.176795	0.203269	10.709	<2e-16 ***
Force		-0.093933	0.011878	-7.908	4.72e-13 ***
Force:rate1		0.017985	0.004537	3.965	0.000112 ***
Force:speed2000		-0.015229	0.005390	-2.825	0.005350 **
Force:speed2500		-0.023562	0.006014	-3.917	0.000134 ***
Force:speed3000		-0.031650	0.006695	-4.728	5.09e-06 ***
Thrust force using weighted mean measure μ_2					
AIC: 203.39	Coefficient	Estimate	Std. Error	t value	p value
(Intercept)		1.874433	0.202963	9.235	<2e-16 ***
Force		-0.070106	0.010812	-6.484	1.15e-09 ***
Force:rate1		0.018868	0.004643	4.064	7.68e-05 ***
Force:speed2000		-0.011676	0.004930	-2.368	0.01911 *
Force:speed2500		-0.019011	0.005603	-3.393	0.00088 ***
Force:speed3000		-0.025598	0.006315	-4.054	7.97e-05 ***
Thrust force using median measure m					
AIC: 179.63	Coefficient	Estimate	Std. Error	t value	p value
(Intercept)		2.076962	0.179865	11.547	<2e-16 ***
Force		-0.078189	0.009387	-8.330	4.14e-14 ***
Force:rate1		0.015360	0.003865	3.974	0.000108 ***
Force:speed2000		-0.013011	0.004614	-2.820	0.005441 **
Force:speed2500		-0.019966	0.005102	-3.914	0.000136 ***
Force:speed3000		-0.027073	0.005671	-4.774	4.17e-06 ***

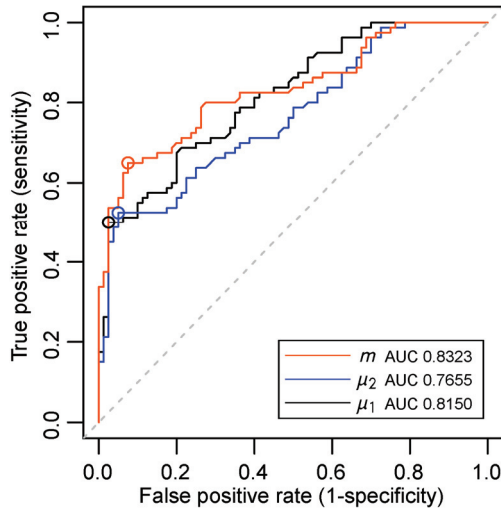


Fig. 7. ROC curve for the logistic models

The ability of these logistic models to estimate the type of bone is illustrated in their ROC curves [10], shown in Fig. 7. The area under the curve (AUC) is 0.832 in the best case, using the median measure, and thus the accuracy of the prediction based on the model is good [18], [21].

Taking the Youden index [24] as the optimal threshold for bone type recognition (circles in Fig. 7), the classification matrices are shown in Table 2 for all 160 bone specimens (TN = true negative, FN = false negative, FP = false positive and TP = true positive). The models using thrust force measures μ_1 and μ_2 misclassified a total of 42 specimens, while 118 specimens were classified correctly (73.75%). Using the median, 78.75% of the bones are correctly classified. These results confirm the assessment made based on the AUC measure, that the accuracy of the prediction is good.

Table 2. Classification matrices

μ_1	Actual 0	Actual 1
Predicted 0	TN = 78	FN = 40
Predicted 1	FP = 2	TP = 40
μ_2	Actual 0	Actual 1
Predicted 0	TN = 76	FN = 38
Predicted 1	FP = 4	TP = 42
m	Actual 0	Actual 1
Predicted 0	TN = 74	FN = 28
Predicted 1	FP = 6	TP = 52

As a conclusion of this statistical analysis, we can affirm that the thrust forces required to drill these two specimen types (bovine bones and porcine bones) are

different [1]. However, it is not possible to distinguish accurately between both specimens based on the force measurements.

4.2. Material recognition

To discriminate material type (bone vs. resin) the observed outcome for the dependent variable is 0 for the photopolymer material (FullCure 720) and 1 for the bone specimens (bovine or porcine bone). Again, the logistic models estimate the probability of the binary response based on one main predictor, thrust force, and the interactions between the thrust force and the feed rate on the one hand, and the thrust force and the rotational speeds on the other, are introduced separately.

Using the weighted mean μ_2 as the thrust force, the ROC curve exhibits the ideal shape, where the upper left corner lies on coordinate (0,1) and the AUC measure takes the maximum value (AUC = 1.0). Thus, it is possible to perform a perfect discrimination between the two materials using this thrust force measure. However, using the mean and the median, μ_1 and m , the upper left corner of the ROC curve lies on coordinate (0,0.9944) and the AUC measure is AUC = 0.9998.

Taking the Youden index as threshold, the classification matrices are shown in Table 3 for all 320 tests. As expected, all the experiments are classified correctly using μ_2 . However, one bone has been classified as FullCure 720 using μ_1 or m .

Table 3. Classification matrices

μ_1	Actual 0	Actual 1
Predicted 0	TN = 160	FN = 1
Predicted 1	FP = 0	TP = 159
μ_2	Actual 0	Actual 1
Predicted 0	TN = 160	FN = 0
Predicted 1	FP = 0	TP = 160
m	Actual 0	Actual 1
Predicted 0	TN = 160	FN = 1
Predicted 1	FP = 0	TP = 159

The boxplots depicted in Figs. 5 and 6 use the weighted mean μ_2 . For this measure, there is no overlap between bones and FullCure 720 at each operational condition of feed rate and rotational speed. The mean and the median values also exhibit this characteristic. Thus, the absence of overlap does not neces-

sarily imply that 100% success in the classification can be achieved.

4.3. Model enhancement

Three different measures of the central tendency of the thrust force profiles have been used in the statistical models: the arithmetic mean, a weighted mean and the median. Although these measures get different classification results, there is no clear evidence that makes us recommend one of them in particular. In this section, we would like to discuss if it possible to enhance the logistic regression models with other measure that is not correlated with the central tendency.

The forces commanded for the porcine specimen shown in Fig. 3 have a greater dispersion around the central tendency measure than in the case of the bovine bone. If this is a common behavior to porcine and bovine records, the value of the standard deviation σ could be added to the linear model to predict the type of bone. The proposed model is:

$$\begin{aligned} y \sim & \beta_0 + \beta_1 f + \beta_2(f \times \omega_r) + \beta_3(f \times v_r) \\ & + \beta_4 \sigma + \beta_5(\sigma \times \omega_r) + \beta_6(\sigma \times v_r). \end{aligned} \quad (5)$$

In Table 4 the coefficients and p values of the model using the arithmetic mean μ_1 for the thrust force and the standard deviation σ , which can also be affected by the rotational speed and the feed rate, were shown. The models using the other two force measures have AIC values of 134.14 (μ_2) and 107.13 (m).

The ROC curves of the logistic models are shown in Fig. 8. The optimal threshold using the Youden index is depicted in circles. Now, the area under the curves are around 95%, which is a very good result for diagnosis. The classification matrices (Table 5)

also confirm this result: 90% of the bones are classified correctly using the median measure for the thrust force and the standard deviation for the dispersion of the force during the drilling process.

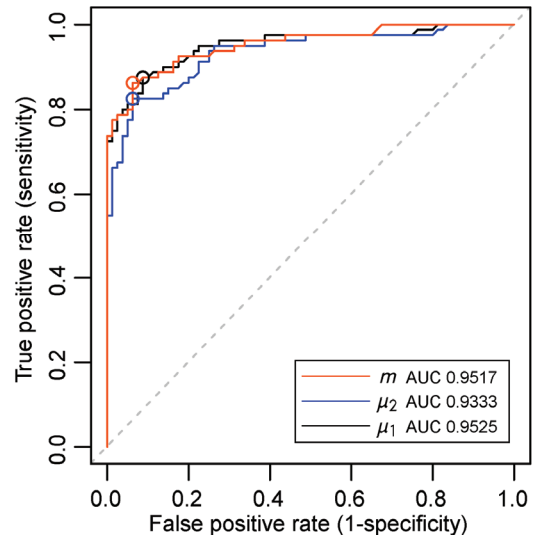


Fig. 8. ROC curve for the logistic models

Table 5. Classification matrices

μ_1 and σ	Actual 0	Actual 1
Predicted 0	TN = 73	FN = 10
Predicted 1	FP = 7	TP = 70

μ_2 and σ	Actual 0	Actual 1
Predicted 0	TN = 75	FN = 14
Predicted 1	FP = 5	TP = 66

m and σ	Actual 0	Actual 1
Predicted 0	TN = 75	FN = 11
Predicted 1	FP = 5	TP = 69

Table 4. Coefficients and p values of the model

AIC: 115.18	Thrust force using mean measure μ_1			
Coefficient	Estimate	Std. Error	t value	p value
(Intercept)	1.53938	0.17315	8.890	1.86e-15 ***
Force	-0.19678	0.02657	-7.407	8.90e-12 ***
Stdev	0.46557	0.08710	5.346	3.32e-07 ***
Force:rate1	0.07864	0.02845	2.764	0.00643 **
Force:speed2000	-0.05724	0.02797	-2.047	0.04245 *
Force:speed2500	-0.10088	0.03741	-2.697	0.00781 **
Force:speed3000	-0.10719	0.03907	-2.744	0.00682 **
Stdev:rate1	-0.26366	0.09242	-2.853	0.00495 **
Stdev:speed2000	0.15976	0.08663	1.844	0.06717 .
Stdev:speed2500	0.28378	0.11877	2.389	0.01813 *
Stdev:speed3000	0.29631	0.12562	2.359	0.01963 *

The three models that include the standard deviation of the force obtain a perfect discrimination between bones and FullCure 720. None of the bones are classified as resin nor vice versa.

4.4. Comparison with other studies

There is little scientific literature dedicated to the classification and recognition of materials based on drilling forces. Some authors have trained neural networks to recognize five different types of concrete [14]. By increasing the number of interactions of the neural network, a success rate of 95.5% was achieved in the classification of the materials. The system recorded seven measures during the drilling process: thrust force, torque, rotary speed, drill position, penetration rate, and motor inlet and outlet pressures. As the layers of concrete were always in the same relative position, drill position was not used as an input to the neural network. The authors also evaluated the relative discriminatory power of the six parameters, and they found that removing thrust force significantly impairs the network's ability to classify the materials.

In [23], the authors tried to distinguish four different states within the bone (the cortical layer, cortical-transit-cancellous, almost-break-cortical and cancellous states) using multi-sensor information fusion and a support vector machine (SVM) classifier. The adopted signals include force, current, feed speed, rotation speed and deflection of the robotic arm. The method was validated through experiments on pig scapula, and a success rate of 93.1% was achieved.

In other studies, some non-destructive experiments are used instead of drilling the material. In [22], the classification of the surface material is made using a recording tool, with an acceleration sensor, a microphone and force sensing resistors to measure friction while dragging the device over the object's surface. A low-dimensional combination of acceleration, sound, friction and image features as input in a Naive Bayes classifier yields an accuracy of 74% from a set of 69 different surfaces.

As shown in previous results, the proposed method obtains a success rate similar to the state of the art, with the advantage of using only a position sensor.

5. Application

We have implemented the results of this work in a novel hand-held bone drilling device. The DRIBON

system used for the experiments operates with a supporting arm. Once the device is in the right location, the surgeon presses a button and the system automatically drills the bone, stopping before any breakthrough occurs. One of its drawbacks is that the system has to be fixed to the floor or somewhere rigid (e.g., a metallic base plate), making the system bulkier and less portable.

We have developed a newer version (Fig. 9), whose main feature is that it can be held by the surgeon like a common home drilling tool, though it performs the drilling process automatically (feed and stop) when the user presses a button. This enables the surgeon a more agile operation and greater control.



Fig. 9. New DRIBON device and interface

The system has been completely redesigned to obtain a more lightweight and ergonomic device. For precise feed displacement control, a Maxon RE25 motor with a Maxon GP 26B planetary gear (5.4:1 reduction) and a 512 ppr Maxon MR optical encoder were used. To control the rotation of the drill bit, a Maxon EC22 brushless DC motor with a Maxon GP 22C planetary gear (4.4:1 reduction) was selected. A belt linear actuator was used to control the displacement of the drill bit with high-backdrivability, which is key for the success of the layer transition detection method.

This new DRIBON system has a total weight of 1 kg, and it can implement feed rates from 0 to 2 mm/s and rotation speeds from 0 rpm to 5000 rpm. It implements our previous successful method for layer transition detection [2] and the novel bone state awareness method proposed in this paper. The control algorithms are implemented in a National Instruments MyRIO system within a control loop rate of 1 kHz.

For the bone state awareness strategy, the database presented in Chapter 3 was implemented as a look-up table with minimum and maximum ranges of thrust force values, depending on feed rate and drill speed

selected by the surgeon (Table 6). For each selected condition (drill speed and feed rate) all thrust force database values of bovine and pig bones within the 99% confidence interval were gathered and their minimum and maximum values were computed. Mean values have been used as in real-time this is the easiest method to compute the average thrust force value during the process.

The interface developed (Fig. 9) enables surgeons to select the feed rate and drill speed. Once the bone drilling has started, the interface shows a healthy bone message as soon as the thrust force value reaches the minimum database value for the selected drill speed and feed rate. Otherwise an “unhealthy bone” message is displayed so that the surgeon can take action.

Table 6. Healthy minimum and maximum thrust force values for different drilling operation parameters

Rotational speed [rpm]	Feed rate 0.5 mm/s		Feed rate 1 mm/s	
	Min [N]	Max [N]	Min [N]	Max [N]
1500	15.16	19.70	20.15	24.13
2000	13.63	16.77	17.08	20.23
2500	13.03	15.85	15.23	18.32
3000	12.10	14.42	14.32	17.35

6. Conclusions

The results obtained in this work give answer to two main questions: 1) whether it is possible to recognize a bovine bone vs. a porcine bone using thrust force, and 2) whether it is possible to recognize bone material vs. another material (in this case FullCure 720) using thrust force. The answer to the first question is yes, with a relatively high success rate. However, given the high overlap in the required thrust force, we can agree with authors that use bovine and porcine bones (without distinguishing them) to validate their systems and methods, as the bone types are similar from the mechanical point of view. Another question that remains unresolved is to what extent these mechanical properties are similar to those found in human bones. Moreover, the age of the bone may be another serious conditioning factor for the healthy range of thrust forces for a specific bone. The answer to the second question is a definitive yes for the two tested materials. This means that it should be easy to detect bone weakness such as osteoporosis from thrust force measures.

Rotational speed and feed rate parameters were found to have a strong statistical significance for the

thrust force required during drilling procedures. An increase in feed rate causes an increase in the thrust force, and an increase in the rotational speed decreases the thrust force.

The new version of the DRIBON device, featuring hand-held capabilities, implements the results of this work on its visual interface alerting the surgeon about the properties of the bone being drilled in real-time.

References

- [1] ACCINI F., DÍAZ I., GIL J.J., *Bone recognition during the drilling process*, 6th IEEE RAS/EMBS International Conference on Biomedical Robotics and Biomechatronics, 2016, 305–310, Singapore.
- [2] ACCINI F., DÍAZ I., GIL J.J., *Using an admittance algorithm for bone drilling procedures*, Computer Methods and Programs in Biomedicine, 2016, 123 (1), 150–158.
- [3] AKAIKE H., *Information theory and the maximum likelihood principle*, 2nd International Symposium on Information Theory, 1973, 267–281, Budapest, Hungary.
- [4] ALLOTTA B., BELMONTE F., BOSIO L., DARIO P., *Study on a mechatronic tool for drilling in the osteosynthesis of long bones: tool/bone interaction, modeling and experiments*, Mechatronics, 1996, 6 (4), 447–459.
- [5] AUGUSTIN G., ZIGMAN T., DAVILA S., UDILLJAK T., STAROVESKI T., BREZAK D., BABIC S., *Cortical bone drilling and thermal osteonecrosis*, Clinical Biomechanics, 2012, 27 (4), 313–325.
- [6] BASIAGA M., PASZENDA Z., SZEWCZENKO J., KACZMAREK M., *Numerical and experimental analyses of drills used in osteosynthesis*, Acta of Bioengineering and Biomechanics, 2011, 13 (4), 29–36.
- [7] BOIADJIEV G., KASTELOV R., BOIADJIEV T., KOTEV V., DELCHEV K., ZAGURSKI K., VITKOV V., *Design and performance study of an orthopaedic surgery robotized module for automatic bone drilling*, The International Journal of Medical Robotics and Computer Assisted Surgery, 2013, 9 (4), 455–463.
- [8] COULSON C., REID A., PROOPS D., *A cochlear implantation robot in surgical practice*, 15th International Conference on Mechatronics and Machine Vision in Practice, 2008, 173–176, Auckland, New Zealand.
- [9] DÍAZ I., GIL J.J., LOUREDO M., *Bone drilling methodology and tool based on position measurements*, Computer Methods and Programs in Biomedicine, 2013, 112 (2), 284–292.
- [10] FAWCETT T., *An introduction to ROC analysis*, Pattern Recognition Letters, 2006, 27(8), 861–874.
- [11] GLAUSER D., FLURY P., VILOTTE N., C.W., B., *Conception of a robotic dedicated to neurosurgical operations*, Fifth International Conference on Advanced Robotics, 1991, 899–904, Pisa, Italy.
- [12] HSU Y.-L., LEE W.-Y., LIN H.-W., *A modular mechatronic system for automatic bone drilling*, Biomedical Engineering, Applications, Basis and Communications, 2001, 13 (4), 168–174.
- [13] KASTELOV R., BOIADJIEV G., BOIADJIEV T., DELCHEV K., ZAGURSKI K., GUEORGUIEV B., *Automatic bone drilling using a novel robot in orthopedic trauma surgery*, Journal of Biomedical Engineering and Informatics, 2017, 3 (2), 62.

- [14] LABELLE D., BARES J., NOURBAKHSH I., *Material classification by drilling*, 17th International Symposium on Automation and Robotics in Construction, 2000.
- [15] LEE W.-Y., SHIH C.-L., *Force control and breakthrough detection of a bone drilling system*, IEEE International Conference on Robotics and Automation, 2003, 1787–1792, Taipei, Taiwan.
- [16] LEE W.-Y., SHIH C.-L., *Control and breakthrough detection of a three-axis robotic bone drilling system*, Mechatronics, 2006, 16, 73–84.
- [17] LOUREDO M., DÍAZ I., GIL J.J., *A robotic bone drilling methodology based on position measurements*, IEEE RAS/EMBS International Conference on Biomedical Robotics and Biomechatronics, 2012, 1155–1160, Roma, Italy.
- [18] METZ C.E., *Basic principles of ROC analysis*, Seminars in Nuclear Medicine, 1978, 8 (4), 283–298.
- [19] PANDEY R.K., PANDA S.S., *Modelling and optimization of temperature in orthopaedic drilling: An in vitro study*, Acta of Bioengineering and Biomechanics, 2014, 16 (1), 107–116.
- [20] PAU H.W., JUST T., BORNITZ M., LASURASHVILLI N., ZAHNERT T., *Noise exposure of the inner ear during drilling a cochleostomy for cochlear implantation*, The Laryngoscope, 2007, 117, 535–540.
- [21] PINES J.M., CARPENTER C.R., RAJA A.S., SCHUUR J.D., *Evidence-Based Emergency Care: Diagnostic Testing and Clinical Decision Rules*, John Wiley & Sons, second edition, 2012.
- [22] STRESE M., SCHUWERK C., IEPURE A., STEINBACH E., *Multi-modal featurebased surface material classification*, IEEE Transactions on Haptics, 2017, 10 (2), 226–239.
- [23] WANG Y., DENG Z., SUN Y., YU B., ZHANG P., HU Y., ZHANG J., *State detection of bone milling with multi-sensor information fusion*, IEEE Conference on Robotics and Biomimetics, 2015, Zhuhai, China.
- [24] YOUDEN W.J., *An index for rating diagnostic tests*, Cancer, 1950, 3, 32–35.